

Electron Density and Anharmonic Thermal Atomic Vibrations in $K_{1-x}Li_xTaO_3$ ($x=0, 0.05, 0.15$) Perovskites *

E. A. Zhurova¹, V. E. Zavodnik², S. A. Ivanov², P. P. Syrnikov³, and V. G. Tsirelson¹

¹ Mendeleev Institute of Chemical Technology, Moscow, Russia

² Karpov Institute of Physical Chemistry, Moscow, Russia

³ Ioffe Physical Technical Institute, Sankt-Petersburg, Russia

Z. Naturforsch. **48a**, 25–28 (1993); received November 8, 1991

The results of accurate X-ray diffraction studies of $KTaO_3$, $K_{0.95}Li_{0.05}TaO_3$ and $K_{0.85}Li_{0.15}TaO_3$ crystals are presented. Anharmonicity of the thermal motion of the oxygen atoms and deformation electron density maps are discussed.

Key words: Anharmonic thermal vibrations; Electron density; Chemical bond.

Perovskite $KTaO_3$ belongs to the class of virtual ferroelectrics that possess ferroelectric properties under external influence (such as electric field, mechanical stress, etc.) or after inclusion of small amounts of impurities. Substitution of K ions by Li ions in crystalline $KTaO_3$ results in a phase transition. As the mechanism of such phase transitions is mainly defined by anharmonic thermal atomic vibrations and by peculiarities of chemical bonds in perovskite-type crystals (Lines and Glass [1]), it is interesting to investigate the latter in $K_{1-x}Li_xTaO_3$ samples. We report the results of a high-precision X-ray diffraction study of three different specimens with the compositions $KTaO_3$ **1**, $K_{0.95}Li_{0.05}TaO_3$ **2** and $K_{0.85}Li_{0.15}TaO_3$ **3**.

The details of the X-ray diffraction experiments with all specimens are given in Table 1. Transparent $K_{1-x}Li_xTaO_3$ single crystals have been grown by spontaneous crystallization from their melt by a method owing to one of the authors (P.P.S.). The mean chemical composition and concentrations of impurities were controlled using a microanalyzer CAMEBAX-301. No impurities were found in the samples within the accuracy limits of the measurement. A ferroelectric phase transition is usually observed in imperfect $KTaO_3$ crystals, but no transition was found in pure $KTaO_3$ crystals (Buzin et al. [2]). The mean concentrations of Li were estimated from the compositions of the melts.

* Presented at the Sagamore X Conference on Charge, Spin, and Momentum Densities, Konstanz, Fed. Rep. of Germany, September 1–7, 1991.

Reprint requests to Prof. Dr. Vladimir G. Tsirelson, Mendeleev Institute of Chemical Technology, Miusskaja pl. 9, Moscow 125 190, Russia.

For the refinements of the $K_{1-x}Li_xTaO_3$ crystal structures using the independent-atom model, scattering factors from the International Tables 1974 [3] were used. For the description of thermal motion the Gram–Charlier expansion of the anharmonic temperature factor $T(q)$ was used [3]:

$$T^{GC}(q) = T^{harm}(q) \left\{ 1 + \frac{(2\pi i)^3}{6} c^{pqr} h_p h_q h_r + \frac{(2\pi i)^4}{24} d^{pqrs} h_p h_q h_r h_s + \dots \right\}, \tag{1}$$

where $T^{harm}(q)$ is the usual harmonic temperature factor, $h_i = h, k, l$, and c^{pqr} and d^{pqrs} are anharmonic

Table 1. The details of X-ray diffraction experiments for $K_{1-x}Li_xTaO_3$ crystals (space group Pm3m).

Details	Crystal 1	Crystal 2	Crystal 3
Mean concentration of Li atoms x	0	0.05	0.15
Radius of spherical specimen, mm	0.056 (2)	0.081 (1)	0.050 (2)
Diffractometer	CAD-4	CAD-4	CAD-4
Radiation	MoK α , β -filter		
Range of $\theta/2\theta$ scan, degrees	2	2	2
Number of measured reflections	2183	2086	2357
Averaging of equivalent reflections	+	+	+
$R_{int} = \Sigma(I_m - I_j)/\Sigma I_j$	0.020	0.015	0.014
Number of independent reflections	148	148	148
$(\sin \theta/\lambda)_{max}, \text{\AA}^{-1}$	1.27	1.27	1.27
Corrections for absorption	+	+	+
TDS	+	+	+
Unit cell parameter, \AA	3.9883 (2)	3.9879 (4)	3.9857 (2)

0932-0784 / 93 / 0100-0025 \$ 01.30/0. – Please order a reprint rather than making your own copy.



Dieses Werk wurde im Jahr 2013 vom Verlag Zeitschrift für Naturforschung in Zusammenarbeit mit der Max-Planck-Gesellschaft zur Förderung der Wissenschaften e.V. digitalisiert und unter folgender Lizenz veröffentlicht: Creative Commons Namensnennung-Keine Bearbeitung 3.0 Deutschland Lizenz.

Zum 01.01.2015 ist eine Anpassung der Lizenzbedingungen (Entfall der Creative Commons Lizenzbedingung „Keine Bearbeitung“) beabsichtigt, um eine Nachnutzung auch im Rahmen zukünftiger wissenschaftlicher Nutzungsformen zu ermöglichen.

This work has been digitalized and published in 2013 by Verlag Zeitschrift für Naturforschung in cooperation with the Max Planck Society for the Advancement of Science under a Creative Commons Attribution-NoDerivs 3.0 Germany License.

On 01.01.2015 it is planned to change the License Conditions (the removal of the Creative Commons License condition “no derivative works”). This is to allow reuse in the area of future scientific usage.

Table 2. Results of $K_{1-x}Li_xTaO_3$ structure refinements: $x = 0$ (crystal 1; column I: extinction parameters refined with all reflections, column II: high-extinction reflections excluded from the refinements), $x = 0.05$ (crystal 2) and $x = 0.15$ (crystal 3).

Parameters	Crystal 1		Crystal 2	Crystal 3
	I	II		
K ⁺ :				
occup.	1.000 (1)	1.000 (1)	0.979 (3)	0.919 (4)
<i>x</i>	1/2	1/2	1/2	1/2
<i>U</i> , Å ²	0.0077 (2)	0.0081 (2)	0.0072 (2)	0.0074 (3)
<i>d</i> ₁₁₁₁ · 10 ⁴	0.0002 (5)	0.0010 (6)	0.0000 (5)	0.0016 (9)
<i>d</i> ₁₁₂₂ · 10 ⁴	0.0002 (2)	0.0004 (2)	0.0000 (2)	0.0000 (3)
Li ⁺ :				
occup.	—	—	—	0.081*
<i>x</i> = <i>z</i>	—	—	—	1/2
<i>y</i>	—	—	—	0.1*
<i>U</i> , Å ²	—	—	—	0.006*
Ta ⁺⁵ :				
<i>x</i>	0	0	0	0
<i>U</i> , Å ²	0.0036 (1)	0.0036 (1)	0.0032 (1)	0.0033 (1)
<i>d</i> ₁₁₁₁ · 10 ⁴	−0.0012 (1)	−0.0011 (1)	−0.0013 (1)	−0.0016 (1)
<i>d</i> ₁₁₂₂ · 10 ⁴	−0.0004 (1)	−0.0003 (1)	0.0004 (1)	−0.0006 (1)
O ^{−2} :				
<i>x</i>	1/2	1/2	1/2	1/2
<i>y</i>	0	0	0	0
<i>U</i> ₁₁ , Å ²	0.0027 (6)	0.0028 (7)	0.0025 (6)	0.0020 (9)
<i>U</i> ₂₂ , Å ²	0.0083 (6)	0.0089 (7)	0.0071 (5)	0.0076 (8)
<i>d</i> ₁₁₁₁ · 10 ⁴	−0.0028 (13)	−0.0027 (14)	−0.0028 (13)	−0.0032 (19)
<i>d</i> ₂₂₂₂ · 10 ⁴	0.0004 (14)	0.0016 (17)	−0.0020 (12)	−0.0016 (18)
<i>d</i> ₁₁₂₂ · 10 ⁴	−0.0003 (3)	−0.0001 (4)	−0.0006 (4)	−0.0011 (4)
<i>d</i> ₂₂₃₃ · 10 ⁴	0.0007 (6)	0.0012 (7)	−0.0001 (6)	−0.0014 (7)
<i>R</i> ^{**}	0.0033	0.0035	0.0037	0.0054
<i>R</i> _w ^{**}	0.0037	0.0039	0.0043	0.0060
<i>S</i> ^{**}	1.1478	1.5300	1.2679	1.3073

* Have been fixed.

** Results of high-angle refinements.

atomic thermal parameters. All the calculations have been done with the program PROMETHEUS (Zucker et al. [4]), adapted for ES-1045 and IBM PC computers.

The refinement procedure was the following. First, scale factor, extinction, occupancy of the potassium position and all thermal parameters were refined with all reflections. The general case of Becker-Coppens extinction with Gaussian distribution of mosaic blocks has been chosen for all crystals. Secondly, all parameters, except the thermal ones, were fixed, and the thermal parameters of K, Ta and O were refined using the high-angle reflections ($\sin \theta/\lambda > 0.9 \text{\AA}^{-1}$). Thirdly, the scale factor was calculated with all reflections. For the Li atoms, however, not all parameters could be refined.

The occupancies of lithium positions were chosen as $(1 - x)$, where x is the occupancy of the potassium position. The lithium atom positions were chosen from the analysis of difference electron density maps. The results of the calculations are given in Table 2. The experimental data for crystals No. 2 and No. 3 yield occupancies of K atoms considerably larger than expected. From the composition of the melts we expected to obtain occupancies of the K atom positions of about 0.95 and 0.85 for crystals No. 2 and No. 3, respectively. However, the refinements showed that during the growth of crystals with assigned content of K (or Li) atoms considerable segregation occurs with a resulting gradient of concentration from crystal to crystal within the precipitate from the melt. Thus only the mean concentration in the precipitate corresponds to the expected value.

The effective one-particle potentials of atoms have been calculated with parameters obtained with high-angle thermal vibration parameters. That potential has the form

$$V(x) = -k_B T \ln \{ p(x)/p(x=0) \}, \quad (2)$$

where $p(x)$ is probability density function (PDF), i.e. the Fourier transform of the temperature factor $T(q)$. The potentials obtained for oxygen appeared to be double-well shaped in the [100]-direction (Figure 1). However, such a potential could not be found around the $(\frac{1}{2} 0 0)$ positions of O atoms, because the PDF shows large negative values in this region. In order to elucidate the reason for the occurrence of such a forbidden PDF, the structure factors of the crystal No. 1 (see Table 2) were analysed. We found that only after exclusion of the seven reflections most affected by extinction (100, 110, 111, 200, 211, 220 and 222) from refinement, a physically meaningful double-well potential for O with a barrier of about $54 \pm 25 \text{ meV}$ (Fig. 1, curve 1) is obtained. (The error was calculated neglecting all correlations between parameters.) We have to conclude that our attempt to determine the correct extinction parameters by a refinement with the Becker-Coppens formalism has failed. However, there is no doubt about the existence of a double-well potential for the oxygen atom.

The obtained splitting of the O atom position raises an important question: does the double-well potential reflect the existence of static displacements of O atoms from regular positions in the crystal? The answer to this question can be obtained only by precise diffraction investigations at different temperatures.

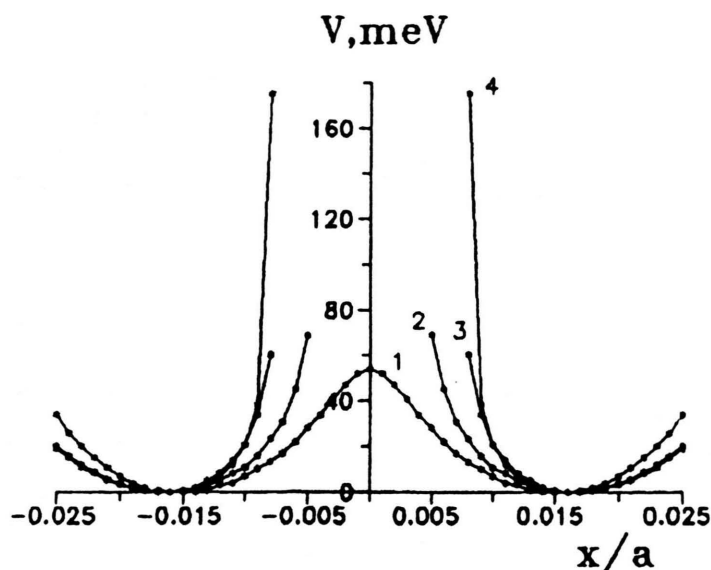


Fig. 1. One-particle potentials of O atoms in [100]-direction. 1 – Crystal No. 1, high-extinction reflections being excluded from the refinements (column II in Table 2). 2 – The same, but extinction parameters being refined with all reflections (column I in Table 2). 3 – The same, but for crystal No. 2. 4 – The same, but for crystal No. 3.

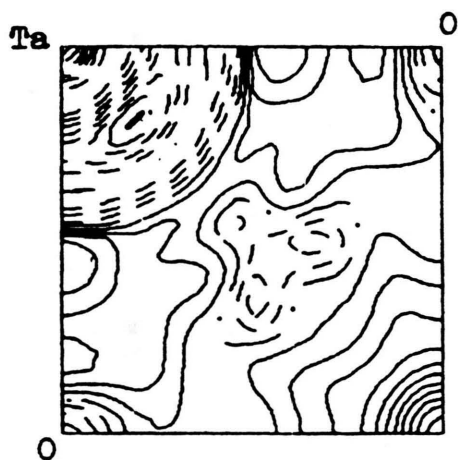


Fig. 2. The deformation electron density map for crystal No. 1, in the $[(001), z=0]$ plane. Contour intervals are $0.1 \text{ e}\text{\AA}^{-3}$. Positive, zero and negative contours are solid, dash-dotted and dashed lines, respectively.

The deformation electron density ($\delta\rho$) maps were then calculated:

$$\begin{aligned} \delta\rho(\mathbf{r}) &= \rho_o(\mathbf{r}) - \rho_c(\mathbf{r}) \\ &= (1/V) \sum_{\mathbf{q}} (F_o(\mathbf{q}) - F_c(\mathbf{q})) \exp(-i\mathbf{q}\mathbf{r}). \end{aligned} \quad (3)$$

The absolute values of experimental coherent structure amplitudes $F_o(\mathbf{q})$ have been derived from X-ray intensities, corrected for extinction and anomalous scattering according to the International Tables [3].

The phases of F_o and structure amplitudes $F_c(\mathbf{q})$ were calculated using spherical atomic scattering factors, and positional and thermal parameters were obtained by high-angle refinements. Calculated in this manner, the $\delta\rho$ -maps characterize the redistribution of electronic charge in the unit cell upon formation of the chemical bonds. One of the $\delta\rho$ -maps obtained is shown in Figure 2. (The other maps are in qualitative agreement with it.) The positive $\delta\rho$ peaks on the Ta–O lines can be assigned to polar covalent σ -bonds between these atoms. The weak positive $\delta\rho$ areas along [110] at a distance of $\sim 1 \text{ \AA}$ from the position of Ta can be associated with an overlapping of π -orbitals of oxygen atoms with $t_{2g}(5d)$ orbitals of the Ta atom. Besides, there are eight positive $\delta\rho$ peaks near the Ta atom in the $\langle 111 \rangle$ -directions. They can be associated with populated atomic $t_{2g}(5d)$ orbitals of the Ta atom. Note that the details vary only weakly with $(\sin \theta / \lambda)_{\text{cut-off}}$, and that they are in close concordance with the deformation electron density in the perovskite-type ReO_3 crystal (Morinaga *et al.* [5]). The peak- $\delta\rho$ at the $(\frac{1}{2} \frac{1}{2} 0)$ -position results from Fourier-series error accumulation on the high-symmetry point.

The Li atoms are manifested on the $\delta\rho$ -maps as the six positive $0.4 \text{ e}\text{\AA}^{-3}$ peaks, shifted along the coordinate axes to a distance of 1.6 \AA from the K atom position. Therefore it can be supposed that these atoms do not occupy vacant positions of K atoms, but are spread out to six different positions in the direc-

tions of crystallographic axes. This supposition is in agreement with the results of NMR studies of van der Klink *et al.* [6].

As can be seen from the $\delta\rho$ -maps, $K_{1-x}Li_xTaO_3$ crystals can be considered as being built up from TaO_6 octahedra with partly covalent chemical bonds. The K^+ ions are located in the holes between these octahedra and interact with the octahedral frame almost electrostatically.

Acknowledgement

We would like to express our gratitude to Prof. H. Schulz for making the program PROMETHEUS available to us, and to an unknown referee for valuable comments. One of us (E.A.Z.) thanks "NPP MOST" for financial support.

- [1] M. E. Lines and A. M. Glass, *Principles and Application of Ferroelectrics and Related Materials*, Clarendon Press, Oxford 1977, p. 736.
- [2] I. M. Buzin, I. V. Ivanov, N. N. Moiseev, and V. F. Chuprakov, *Fiz. Tverd. Tela* **22**, 2057 (1980) and *Sov. Phys. Solid State* **22**, 1200 (1980).
- [3] *International Tables for X-ray Crystallography*. Vol. IV. (N. M. F. Henry and K. Lonsdale, eds.), Kynoch press, Birmingham 1974.
- [4] U. H. Zucker, E. Perenthaler, W. F. Kuhs, R. Bachmann, and H. Schulz, *J. Appl. Cryst.* **16**, 358 (1983).
- [5] M. Morinaga, K. Sato, J. Harada, H. Adachi, S. Ohba, and Y. Saito, *J. Phys. C* **16**, L177 (1983).
- [6] J. J. van der Klink, D. Rytz, F. Borsa, and U. T. Höchli, *Phys. Rev. B* **27**, 89 (1983).